Optimisation of a submarine's resonance changer using the method of moving asymptotes

Sascha Merz (1), Nicole Kessissoglou (1), Roger Kinns (1)[*] Steffen Marburg (2)

(1) School of Mechanical and Manufacturing Engineering, University of New South Wales,
Sydney, NSW 2052 Australia
[*]Senior Visiting Research Fellow
(2) Insititut für Festkörpermechanik, Technische Universität,
Mommsenstr. 13, 01062 Dresden, Germany

ABSTRACT

In order to reduce the sound power radiated by a submarine, the transmission of fluctuating forces from the propeller to the hull can be reduced by implementation of a resonance changer in the propulsion system. A resonance changer acts as a hydraulic vibration absorber and can be modelled as a single degree-of-freedom system with virtual mass, stiffness and damping parameters. However, changing the dynamics of the propeller/shafting system can lead to increased sound radiation from the propeller. A numerical finite element / boundary element model of a submarine has been developed in order to find optimum design parameters for the resonance changer, such that the overall sound power radiated from the hull as well as the propeller is reduced. The global optimum virtual stiffness, damping and mass parameters of the resonance changer have been found by applying the method of moving asymptotes. It is shown that the influence of sound radiation from the propeller is only relevant, if higher harmonics of the blade passing frequency are assumed to have a similar amplitude as the fundamental harmonic of the blade passing frequency.

INTRODUCTION

An important mechanism that causes sound radiation from a submarine is the operation of the propeller in a non-uniform wake (Carlton 1994). This mechanism leads to fluctuating forces correlated to the blade passing frequency (*bpf*) at the propeller hub, leading to sound radiated directly from the propeller and to excitation of the submarine hull through the shaft. The vibration excited by the forces can be correlated to the accordion modes of the pressure hull which are efficient sound radiators (Norwood 1995).

In order to reduce the radiated sound power of a submarine, a fully coupled finite element/boundary element model has been developed to minimise a cost function that represents the radiated sound power over a given frequency range. At low frequencies (< 100 Hz), the fluctuating forces at the propeller are assumed to be harmonic and linear. Hence, the analysis has been conducted in the frequency domain using the Helmholtz equation for the exterior radiation/scattering problem. The submarine is a complex, non-homogeneous structure, but its different parts may be represented by simplified physical models such as shells, rods and spring-mass-damper systems. The numerical approach used here to solve the strong fully coupled structure/fluid problem in the low frequency range, where the densities of the structure and the fluid are of similar order, is the combination of the finite element (FE) method to represent the structure and the boundary element (BE) method to represent the fluid (Zienkiewicz and Taylor 2005, Brebbia and Ciskowski 1991, Amini et al. 1992).

The propeller/shafting system comprises of the propeller, propeller shaft, thrust bearing, foundation and a device known as a resonance changer (RC), which acts as a dynamic hydraulic vibration absorber (Goodwin 1960). Dylejko developed simplified, analytical submarine models to find optimum design parameters for different RC configurations in order to minimise the maximum radiated sound pressure rather than the overall radiated sound power (Dylejko et al. 2007, Dylejko 2008). A genetic optimisation strategy was used for the optimisation process. Due to simplifications in the analytical models such as omission of the tailcone and pressure field from the propeller, the complex interaction between the propeller and the submarine hull was not taken into account.

In contrast to analytical methods, numerical methods allow the development of more detailed and complex structural models. However, the computational cost is much higher and non-gradient based optimisation methods such as genetic algorithms are not viable. Hence, gradient based optimisation techniques are preferred and the sensitivity of the cost function to structural design parameters is computed. In previous work by the authors, the structural and acoustic responses of a submarine were presented for fixed parameters of the RC, where excitation of the submarine hull due to fluid forces was taken into account (Merz et al. 2009a). In this paper, the focus is on optimising the RC parameters of a submarine. Numerical models of the sound power radiated by a submarine are presented, where the sensitivity of the weighted sound power over the relevant frequency range to design parameters of the propeller/shafting system has been computed. The sensitivity is obtained in a semi-analytical way by employing the adjoint operator (Marburg 2002). Optimum parameters are found for the virtual stiffness, damping and mass of the RC by applying the globally convergent method of moving asymptotes (Svanberg 2002).

DYNAMIC MODEL OF THE SUBMARINE

A dynamic model to describe the low frequency structural and acoustic responses of a submarine has been presented previously by the authors (Merz et al. 2009a). The pressure hull was modelled as a thin-walled cylinder with evenly spaced ring-stiffeners of rectangular cross-section and two evenly spaced circular plates that represent the bulkheads. As the end plates of a submarine pressure hull are stiff in comparison to other parts, they have been modelled as rigid plates. In order to account for the contribution of the on-board machinery and internal structure to the dynamic behaviour of the submarine, a distributed mass has been attached to the cylindrical shell of the pressure hull (Tso and Jenkins 2003). The submarine model is shown in Fig. 1.

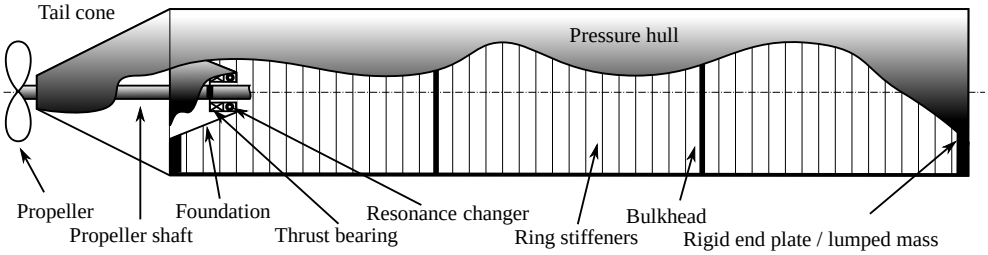

Figure 1: Submarine hull

The propeller/shafting system was modelled in a modular manner as shown in Fig. 2 (Dylejko et al. 2007), where the propeller force and velocity amplitude are given by f_p and v_p, respectively. The hull drive point force and velocity are denoted by f_h and v_h. The propeller as well as the added mass effect of the surrounding water for the propeller are represented by a lumped mass m_p. The propeller dimensions for calculating the propeller mass and the fluid loading effect are chosen by assuming that the propeller volume is $1/1000$ of the volume displaced by the pressure hull. The propeller diameter is assumed to be half the pressure hull diameter. The propeller shaft was modelled as a simple rod with an effective length l_se and an overall length l_s as shown in Fig. 2, where the overhang was represented by a lumped mass. The shaft properties are also defined by its cross-sectional area A_s, Young's modulus E_s and density ρ_s. The thrust bearing was assumed to act as a spring-mass-damper system with mass m_b, damping coefficient c_b and spring constant k_b. The resonance changer is located between the thrust bearing and the foundation as shown in Fig. **??** and has been modelled as a spring-mass-damper system according to Goodwin (1960). The RC is represented by virtual mass, damper and spring parameters, which are calculated by (Goodwin 1960)

$$m_\mathrm{r} = \frac{\rho_\mathrm{r} A_0^2 L}{A_1}; \qquad c_\mathrm{r} = 8\pi\mu L \frac{A_0^2}{A_1^2}; \qquad k_\mathrm{r} = \frac{A_0^2 B}{V}. \tag{1}$$

ρ_r is the density of the hydraulic medium, μ is the dynamic viscosity and B is the bulk modulus of the oil in the RC. V is the volume of the reservoir, A_1 is the cross-sectional area of the pipe, L is the pipe length and A_0 is the cross-sectional area of the cylinder. The foundation is simplified as a truncated cone for the axisymmetric model with end radii a and b as shown in Fig. 2. The Young's modulus, density, Poisson's ratio and thickness of the foundation are given by E_f, ρ_f, ν_f and h_f, respectively.

COUPLED FE/BE MODEL

In this work, the radiated sound power from a coupled vibro-acoustic system with additional discrete sources in the fluid domain has been evaluated. This was accomplished by representing the structure using finite elements and representation of the fluid using boundary elements, where strong coupling is considered at the structure/fluid interface (Merz et al. 2009a). Strong coupling involves the acoustic medium influencing the dynamic behaviour of the structure, as the densities of fluid and structure are of similar order. Under the assumption that an acoustically hard surface is present, the continuity condition requires that the displacement of the fluid equals the displacement of the structure normal to the surface. In addition, the pressure of the fluid results in an external distributed force on the structure normal to the surface. The combined problem is mathematically expressed as

$$\mathbf{S}(\omega)\mathbf{x}(\omega) = \mathbf{y}(\omega), \tag{2}$$

where the linear operator **S** is composed of the BE and FE system matrices and the geometric coupling matrices. The unknown vector **x** contains the nodal displacements of the FE model as well as the acoustic pressure in the collocation points for the BE model, and can be found by formally inverting **S**. The vector **y** represents the exciting structural forces and contributions from fixed sources in the acoustic domain. ω is the radian frequency. For the models presented in this work, non-matching meshes have been used. This requires a piecewise relaxation of the continuity condition by means of Mortar elements (Belgacem 1999).

SOUND FIELD RADIATED BY THE PROPELLER

An analytical model for the sound field radiated by the propeller is presented in Merz et al. (2009a). The sound field is the combination of contributions from (i) the hydrodynamic mechanism that arises from the propeller operating in a non-uniform wake and (ii) the axial fluctuation of the propeller due to vibration of the propeller/shafting system. The sound radiation that corresponds to the axial force on the propeller hub is given by the dipole

$$p(r,\theta) = \mathrm{j}k\mathrm{g}(r) f \left(1 - \frac{\mathrm{j}}{kr}\right) \mathrm{D}(\theta), \tag{3}$$

where k is the fluid wave number, θ is the angle between the field point direction and the force direction, f is the amplitude of the exciting force, r is the distance between the source and the field point, $\mathrm{D}(\theta) = \cos\theta$ is the directivity function and

$$\mathrm{g}(r) = \frac{\mathrm{e}^{-\mathrm{j}kr}}{4\pi r} \tag{4}$$

is the free space Green's function.

The contribution due to (ii) resulting from vibration of the propeller can be computed using a rigid disc approximation. The pressure is also given by equation (3) and the directivity function is (Morse and Ingard 1968)

$$\mathrm{D}(\theta) = \frac{2\mathrm{J}_1(ka\sin\theta)}{ka\cos\theta} \approx \cos\theta, \text{ small } ka, \tag{5}$$

where J_1 is the first order Bessel-function and a is the disc radius. The force acting on the fluid is obtained in terms of the axial propeller velocity v_p by

$$f = 2sz_\mathrm{c}z_\mathrm{a}v_\mathrm{p}, \tag{6}$$

where $s = \pi a^2$ is the area of the disc surface, z_c is the characteristic impedance of the fluid and z_a is the radiation impedance. The radiation impedance can be expressed as the sum of its real and imaginary parts, corresponding to the resistance r_a and the reactance x_a, respectively. The resistance and reactance can be obtained under the assumption that a freely suspended disc reveals twice the admittance of a disc in an infinite baffle (Mellow and Kärkkäinen 2005). For small ka, this gives

$$r_\mathrm{a} = \frac{8(ka)^4}{27\pi^2}, \quad x_\mathrm{a} = \frac{4ka}{3\pi}. \tag{7}$$

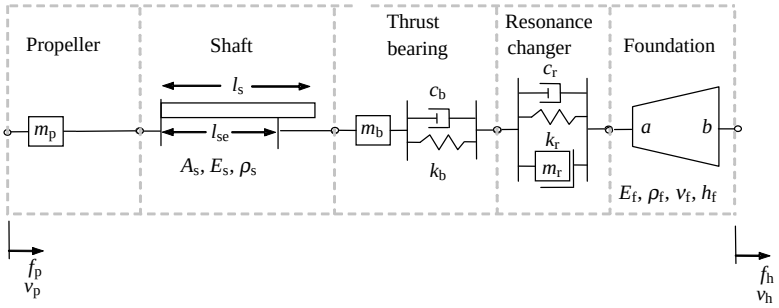

Figure 2: Propeller/shafting system (Dylejko et al. 2007)

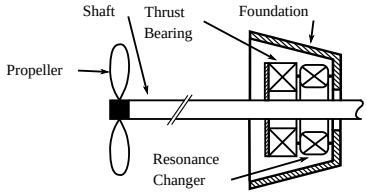

Figure 3: Detail of the propeller/shafting system

SENSITIVITY OF THE RADIATED SOUND POWER

The sound power radiated through a surface Λ is given by (Wu 2000)

$$\Pi(\omega) = \frac{1}{2}\int_{\Lambda} p(\omega)v^*(\omega)\mathrm{d}\Lambda, \tag{8}$$

where p is the acoustic pressure of the fluid and v is the normal velocity of a fluid particle at the surface. As the radiated sound power of the discrete sources in the fluid domain is not implicitly known, a surface enclosing the sources and the structure has to be chosen in order to evaluate the overall radiated sound power. If the surface Λ is spherical and in the far-field with respect to the sound sources, then equation (8) simplifies to (Ross 1987)

$$\Pi(\omega) \approx \frac{1}{2\rho c}\int_{\Lambda} p(\omega)p^*(\omega)\mathrm{d}\Lambda, \tag{9}$$

where ρ is the density of the fluid and c is the speed of sound. The sound pressure can be expressed as a piecewise interpolation, where the pressure is given at a set of discrete points. For the purpose of integration, Gaussian integration points are chosen to interpolate the pressure. A discrete version of equation (9) is obtained by considering the fluid and geometry properties of the surface Λ in a matrix

$$\Pi(\omega) = \mathbf{p}^{\mathrm{H}}(\omega)\boldsymbol{\Theta}\mathbf{p}(\omega). \tag{10}$$

If $\mathbf{x}$ is known, then the vector of discrete pressures $\mathbf{p}$ on the surface Λ can be explicitly obtained by (Merz et al. 2009b)

$$\mathbf{p}(\omega) = \mathbf{T}(\omega)\mathbf{x}(\omega) + \mathbf{p}_{\mathrm{inc}}(\omega). \tag{11}$$

The transfer matrix $\mathbf{T}$ is obtained by integration over the vibrating surface of the structure and $\mathbf{p}_{\mathrm{inc}}$ represents the pressure contribution from discrete sources in the fluid domain at the integration points of the surface Λ.

The sensitivity of the radiated sound power to a set of structural design parameters ϑ of the vibrating structure, that do not have an influence on the scatterer's surface geometry, is obtained by differentiation of equation (10). Omitting the ω dependence, differentiating equation (10) gives

$$\frac{\partial \Pi}{\partial \vartheta} = 2\mathbf{p}^{\mathrm{H}}\boldsymbol{\Theta}\frac{\partial \mathbf{p}}{\partial \vartheta}. \tag{12}$$

The sensitivity of the pressure at the integration points with respect to the design parameters is obtained by differentiation of equation (11), and is given by

$$\frac{\partial \mathbf{p}}{\partial \vartheta} = \mathbf{T}\frac{\partial \mathbf{x}}{\partial \vartheta}. \tag{13}$$

In order to obtain an expression for the sensitivity of the vector $\mathbf{x}$ with respect to the design parameters, equation (2) has to be differentiated which yields

$$\mathbf{S}\frac{\partial \mathbf{x}}{\partial \vartheta} + \frac{\partial \mathbf{S}}{\partial \vartheta}\mathbf{x} = \frac{\partial \mathbf{y}}{\partial \vartheta}. \tag{14}$$

Equation (14) can then be reordered such that an expression for the sensitivity of the vector $\mathbf{x}$ with respect to the design parameters is obtained and is given by

$$\frac{\partial \mathbf{x}}{\partial \vartheta} = \mathbf{S}^{-1}\left(\frac{\partial \mathbf{y}}{\partial \vartheta} - \frac{\partial \mathbf{S}}{\partial \vartheta}\mathbf{x}\right). \tag{15}$$

In order to compute the sensitivity of the sound power, equations (12), (13) and (14) can be combined in an adjoint operator formulation (Marburg 2002)

$$\frac{\partial \Pi}{\partial \vartheta} = 2\mathbf{p}^{\mathrm{H}}\boldsymbol{\Theta}\mathbf{T}\mathbf{S}^{-1}\left(\frac{\partial \mathbf{y}}{\partial \vartheta} - \frac{\partial \mathbf{S}}{\partial \vartheta}\mathbf{x}\right). \tag{16}$$

Let $\mathbf{b}^{\mathrm{T}} = 2\mathbf{p}^{\mathrm{H}}\boldsymbol{\Theta}\mathbf{T}$ and $\mathbf{z}^{\mathrm{T}} = \mathbf{b}^{\mathrm{T}}\mathbf{S}^{-1}$, then the sensitivity of the sound power can be found for any set of parameters ϑ, as long as the solution of the system of equations $\mathbf{S}^{\mathrm{T}}\mathbf{z} = \mathbf{b}$ is known. This means that for an arbitrary number of structural design parameters, only two systems of equations have to be solved.

OPTIMISATION

For optimisation of the resonance changer parameters, the following cost function has been defined to represent the radiated sound power over the frequency range of interest (Marburg 2002)

$$J = \frac{1}{\Delta\omega}\int_{\omega} \Pi(\omega)\mathrm{d}\omega. \tag{17}$$

The gradient of the cost function can be obtained by differentiating equation (17) with respect to the design parameters ϑ, and is given by

$$\frac{\partial J}{\partial \vartheta} = \frac{1}{\Delta\omega}\int_{\omega} \frac{\partial \Pi(\omega)}{\partial \vartheta}\mathrm{d}\omega. \tag{18}$$

The problem of minimising the radiated sound power can be written as

$$\begin{aligned} &\text{minimise } J(\vartheta), \\ &\text{subject to } \quad \underline{\vartheta} \le \vartheta \le \overline{\vartheta}, \end{aligned} \tag{19}$$

where $\underline{\vartheta}$ and $\overline{\vartheta}$ are the lower and upper bounds for the design parameters, respectively. As the first derivatives of the cost

function J with respect to the design parameters ϑ are explicitly available, an appropriate family of methods to find local minima are the quasi-Newton algorithms (Haftka and Gurdal 1992). An example of such an algorithm that is applicable to equation (19) is the limited memory Broyden–Fletcher–Goldfarb–Shanno algorithm with parameter bounds (L-BFGS-B) (Byrd et al. 1995). However, applying the L-BFGS-B directly to equation (19) can require a large number of computationally expensive cost function evaluations. In addition, the process can get easily trapped in a numerically related local minimum. In order to reduce the number of required evaluations of J and $\frac{\partial J}{\partial \vartheta}$, an iterative algorithm can be applied, where the problem is locally approximated by an explicit subproblem

$$\begin{aligned} &\text{minimise } F(\vartheta)^{(k)}, \\ &\text{subject to } \quad \underline{\vartheta}^{(k)} \leq \vartheta \leq \overline{\vartheta}^{(k)}, \end{aligned} \tag{20}$$

for an iteration point k. The subproblem is solved using the L-BFGS-B. The optimum parameters for the subproblem represent the next iteration point and the formulation for the next subproblem is modified based on data from previous iterations. The iteration is stopped when certain convergence criteria are fulfilled. An example for this approach is the method of moving asymptotes (MMA), where asymptotes are used to approximate the cost function (Svanberg 1987). For the algorithm used in this paper, inner iterations l are conducted in addition to the outer iterations k. This approach is called the globally convergent method of moving asymptotes (GCMMA) (Svanberg 2002). The cost function is approximated near the iteration points using

$$F(\vartheta)^{(k,l)} = \sum_{i=1}^{n} \left(\frac{q_i^{(k,l)}}{\vartheta_i^{(k)} - \vartheta_i + \sigma_i^{(k)}} + \frac{r_i^{(k,l)}}{\vartheta_i - \vartheta_i^{(k)} + \sigma_i^{(k)}} - \frac{q_i^{(k,l)} + r_i^{(k,l)}}{\sigma_i^{(k)}} \right) + J(\vartheta^{(k)}) \tag{21}$$

where n represents the number of parameters, i is the index for a parameter, $\vartheta^{(k)}$ represents the optimal solution from the last outer iteration step and $\sigma^{(k)}$ are the moving asymptotes. The asymptotes are moved after each outer iteration. If the process oscillates, the asymptotes are moved closer to the iteration point to make the approximation more conservative. In contrast, if the process is slow, the asymptotes are moved away from the iteration point. The coefficients $q_i^{(k,l)}$ and $r_i^{(k,l)}$ are given by

$$q_i^{(k,l)} = \left(\sigma_i^{(k)}\right)^2 \max\left\{0, \frac{\partial J_i}{\partial \vartheta_i}\left(x^{(k)}\right)\right\} + \frac{\psi^{(k,l)}\sigma_i^{(k)}}{4}, \tag{22}$$

$$r_i^{(k,l)} = \left(\sigma_i^{(k)}\right)^2 \max\left\{0, -\frac{\partial J_i}{\partial \vartheta_i}\left(x^{(k)}\right)\right\} + \frac{\psi^{(k,l)}\sigma_i^{(k)}}{4}, \tag{23}$$

where the parameter $\psi^{(k,l)}$ is adjusted for the inner iteration in order to achieve global convergence. This is accomplished by increasing $\psi^{(k,l)}$ until $J\left(\hat{\vartheta}^{(k,l)}\right)$ is smaller than $F\left(\hat{\vartheta}^{(k,l)}\right)$, where $\hat{\vartheta}^{(k,l)}$ denotes the optimal solution for the subproblem of the inner iteration. Subsequently $\hat{\vartheta}^{(k,l)}$ becomes the next outer iteration point $\vartheta^{(k)}$. Rules for updating the parameters $\sigma^{(k)}$ and $\psi^{(k,l)}$ and for the definition of $\underline{\vartheta}^{(k)}$ and $\overline{\vartheta}^{(k)}$ can be found in Svanberg (2002).

RESULTS

Results are presented for optimisation of the RC virtual damping, stiffness and mass parameters using different cost functions. Results are also given for the sensitivity of some cost functions to these parameters near the optimum. ANSYS 11 was used to generate the FE and BE meshes and to compute the FE stiffness, mass and damping matrices. All other computations were conducted using software implemented in SciPy and C++. For efficient generation of the results, the calculation of the cost function has been parallelised with respect to the frequency using the Message Passing Interface (MPI), by employing a method similar to that described in Miller and Davis (1992). Integration over the frequency range was implemented in an adaptive manner by comparing results for the Simpson rule to results for the trapezium rule. A minimum number of 210 integration points was used. System matrices that are independent of the design parameters have been precomputed and stored in a database at a step size of 0.1 Hz.

Properties of the submarine's propeller/shafting system and hull are given in Tables 1 and 2, respectively. By taking into account physical feasibility as described in Dylejko (2008), the RC virtual damping was varied between 5×10^3 to 1.1×10^6 kg/s. Ranges from 1.5×10^7 to 1.5×10^9 N/m and from 1 to 20 tonnes were chosen for the RC virtual stiffness and mass, respectively.

Table 1: Parameters for the propeller/shafting system

Parameter	Value	Unit
Propeller diameter	3.25	m
Propeller structural mass	10	tonnes
Propeller added mass of water	11.443	tonnes
Shaft Young's modulus	200	GPa
Shaft Poisson's ratio	0.3	
Shaft density	7800	kg/m^3
Shaft cross-sect. area	0.071	m^2
Shaft length	10.5	m
Effective shaft length	9	m
Bearing mass	0.2	tonnes
Bearing stiffness	2×10^{10}	N/m
Bearing damping	3×10^5	kg/s
Resonance changer mass	1	tonne
Foundation major radius	1.25	m
Foundation minor radius	0.52	m
Foundation half angle	15	deg
Foundation thickness	10	mm
Foundation Young's modulus	200	GPa
Foundation density	7800	kg/m^3

Table 2: Parameters for the submarine hull

Parameter	Value	Unit
Cylinder length	45.0	m
Cylinder radius	3.25	m
Shell thickness	0.04	m
Stiffener cross-sectional area	0.012	m^2
Stiffener spacing	0.5	m
Young's modulus of structure without foundation	210	GPa
Young's modulus of foundation	200	GPa
Poisson ratio of structure	0.3	
Density of structure	7800	kg/m^3
Structural loss factor	0.02	
Added mass	796	kg/m^2
Stern lumped mass	188	tonnes
Bow lumped mass	200	tonnes
Cone half angle	24	deg
Cone length	9.079	m
Cone smaller radius	0.3	m
Density of fluid	1000	kg/m^3
Speed of sound	1500	m/s

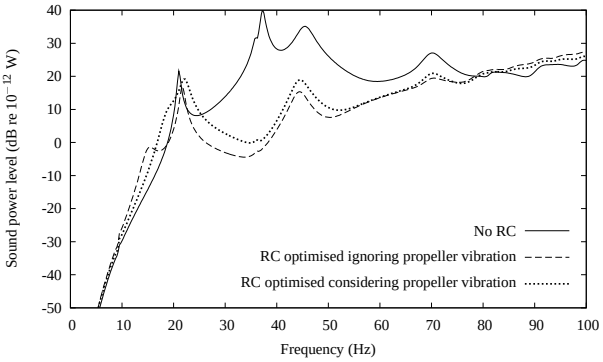

Figure 4: Radiated sound power with and without the use of an RC

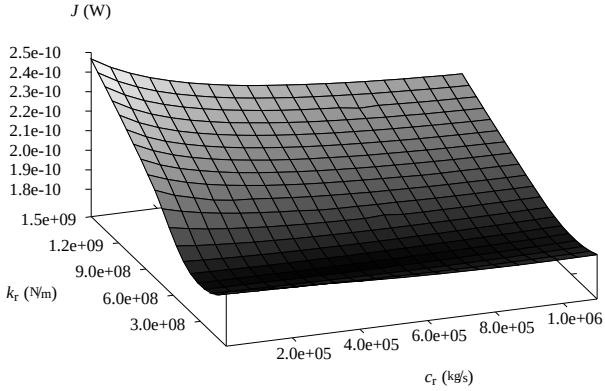

Figure 5: Cost function, when sound radiation due to propeller vibration is neglected

Optimisation

The globally convergent method of moving asymptotes (GCMMA) was used to find optimum design parameters of the resonance changer. Eight different initial parameter sets were used, where the 3-dimensional parameter space was initially subidivided by three, such that the starting sets resulted from the $2 \times 2 \times 2$ intersections. When the cost function values differed by less than 1^{-20} W between two subsequent iterations, convergence was assumed. The computations were obtained using a cluster of six Pentium 4 CPUs at 3 GHz, where an optimisation run required about 40 minutes. Two cost functions according to equation (17) were considered, where for the first cost function, sound radiation due to propeller vibration was neglected and for the second cost function, sound radiation due to propeller vibration has been taken into account. The cost functions were obtained by integration of the sound power due to a force weighted with $(\omega/\Delta\omega)^2$ from 1 to 100 Hz. This is because the force increases proportionally with the square of the propeller rotational velocity.

For the cost function where sound radiation due to propeller vibration has been neglected, six out of the eight sets of initial parameters lead to a common minimum with a function value of around 7.19×10^{-13} W. A global optimum for the RC parameters was found for a cost function value of 7.1865×10^{-13} W, where $c_r = 4.3657 \times 10^5$ kg/s, $k_r = 3.0024 \times 10^8$ N/m and $m_r =$ 1 tonne. For the cost function where sound radiation due to propeller vibration was taken into account, seven out of the eight sets of initial parameters converged to a common minimum, where the cost function value of 2.6745×10^{-13} W was given for $c_r = 1.1 \times 10^6$ kg/s, $k_r = 5.3818 \times 10^8$ N/m and $m_r = 1$ tonne.

Figure 4 shows the radiated sound power, when no RC is implemented, when an optimised RC according to the first cost function is implemented, and when an optimised RC according to the second cost function is implemented. The peaks in the radiated sound power at around 20, 45 and 70 Hz represent the first three hull axial resonances. The maximum sound radiation occurs at the fundamental propeller/shafting system resonance which occurs at around 37 Hz. For the majority of the frequency range, the radiated sound power for a submarine model with no RC is significantly higher than for the submarine model with an RC that has been optimised using any of the cost functions. The curves for the cost functions are similar, but the radiated sound power for the cost function where sound radiation due to propeller vibration has been taken into account is slightly lower for frequencies above about 70 Hz. This is attributed to the fact that the sound radiation in the high frequency range is strongly correlated to propeller vibration. A higher RC virtual damping obtained using the cost function where sound radiation from the propeller has been taken into acount leads therefore to a decrease of radiated sound power at higher frequencies.

Sensitivity analysis

In order to investigate the influence of the RC parameters on the radiated sound power, the sensitivity of the cost functions to the RC virtual damping and stiffness has been investigated. The sensitivity of the cost functions to the RC virtual mass has been omitted as all investigated cost functions resulted in the same RC virtual mass of 1 tonne. This value has also been found previously by Dylejko (2008). Hence, the optimum RC virtual mass parameter of 1 tonne has been used for the sensitivity analyses presented here.

Results for the cost function where sound radiation due to propeller vibration has been neglected is given in Fig. 5. Low values for the cost function are obtained by using small values for the RC virtual stiffness k_r. In this case, the propeller/shafting system becomes more flexible and uncoupled from the hull. The RC virtual damping c_r has only a notable influence for higher values of k_r, when the coupling between the propeller/shafting system and the hull is strong. In this case, an increase of the damping leads to a decrease of the cost function values.

The radiated sound power for the maximum and minimum values of the cost function in Fig. 5 is presented in Fig. 6. It can be seen that for the maximum cost function values, the fundamental propeller/shafting system resonance is detunded to around 27 Hz, but peak sound radiation still occurs. For the minimum cost function value, the fundamental propeller/shafting system resonance is detuned to about 14 Hz and peak sound radiation occurs at higher frequencies above about 80 Hz, where no decrease in radiated sound power can be observed.

The sensitivities of the cost function where sound radiation due to propeller vibration has been neglected, with respect to the RC virtual damping and stiffness, are shown in Figs. 7 and 8, respectively. It can be seen that the minimum cost function value is stable with respect to the RC virtual damping c_r. However, moderate changes of the RC virtual stiffness k_r may lead to an increase of sound radiation.

Results for the cost function where sound radiation due to propeller vibration is taken into account are given in Fig. 9. It can be seen that an increase of the RC virtual damping leads to lower values for J. Two distinct local maxima of the cost function can be identified. The first local maximum occurs at the upper limit for k_r and the lower limit for c_r. The second local maximum occurs at the lower limit for both the RC virtual

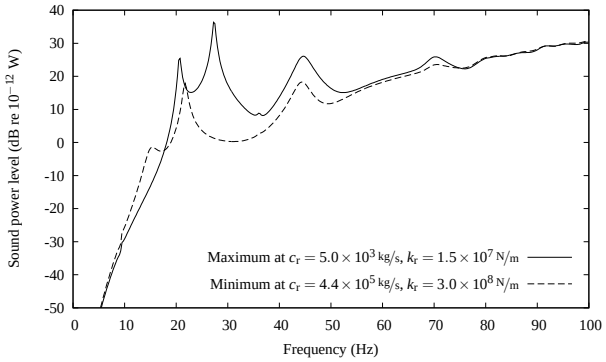

Figure 6: Radiated sound power at the maximum and minimum values of the cost function, when sound radiation due to propeller vibration is neglected

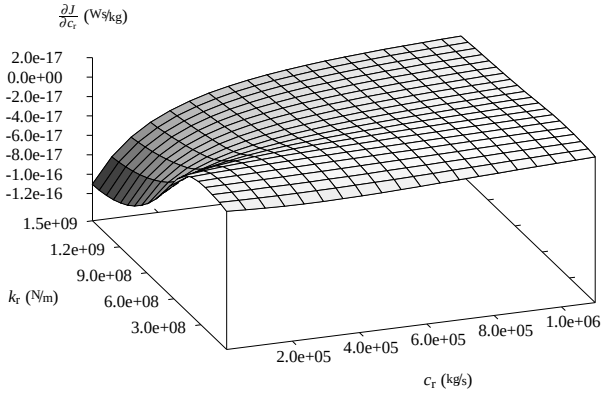

Figure 7: Sensitivity of the cost function when sound radiation due to propeller vibration is neglected, with respect to the virtual damping of the RC

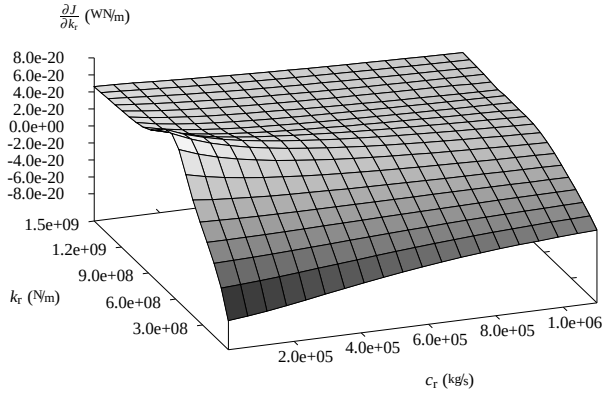

Figure 8: Sensitivity of the cost function when sound radiation due to propeller vibration is neglected, with respect to the virtual stiffness of the RC

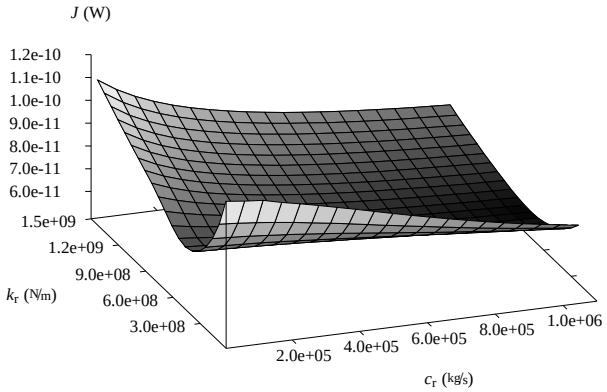

Figure 9: Cost function when sound radiation due to propeller vibration is considered

stiffness k_r and damping c_r. The variation of sound power with frequency is shown in Fig. 10 for the corresponding RC parameters. For the first local maximum, the cost function is dominated by sound radiation at the fundamental propeller/shafting system resonance. In this case, the fundamental resonance of the propeller/shafting system has been decreased from 37 Hz to 27 Hz when compared to the results shown in Fig. 4 with no RC. For the second local maximum, the cost function is dominated by the sound power due to propeller vibration in the high frequency range, since a decrease of the values for c_r and k_r involves an increase of the propeller/shafting system axial flexibility. For the minimum cost function value, the fundamental hull resonance can be barely observed at around 18 Hz. Due to the frequency weighting, the contribution of the radiated sound power to the cost function is small at this frequency.

The sensitivity of the cost function when sound radiated due to propeller vibration is taken into account, with respect to the virtual damping and the virtual stiffness of the resonance changer, is shown in Figures 11 and 12, respectively. The plots are similar to the results for the cost function, when sound radiation due to propeller vibration has been neglected. The major difference occurs for the sensitivity of the cost function with respect to the virtual damping, which is increased for low values of k_r. It can be seen in Fig. 9 that the first maximum of the cost function at the lower limits of the RC parameters is primarily sensitive to the RC stiffness, whereas the second maximum of the cost function at the lower limit of the RC virtual damping and the upper limit of the RC virtual stiffness is primarily sensitive to the RC virtual damping. It can be concluded that an increase in RC virtual stiffness reduces axial propeller vibration in the higher frequency range. An increase in RC virtual damping will primarily lower sound radiation at the propeller/shafting system fundamental resonance.

CONCLUSIONS

Optimum design parameters for a passive vibration attenuation device known as a resonance changer have been found using a fully coupled vibro-acoustic model for a submarine. The overall radiated sound power in the low frequency range has been minimised, where sound radiated from the hull as well as sound radiated from the propeller has been taken into account. Cost functions have been obtained by integration of the frequency-weighted radiated sound power over the frequency range of interest. In order to use gradient based optimisation, the sensitivity of the cost function to the design parameters was also computed using an adjoint operator formulation. The globally convergent method of moving asymptotes has been applied in conjunction with the L-BFGS-B method to find the optimum virtual damping, stiffness and mass parameters for the resonance changer. With respect to the parameter space, eight equally distributed initial parameter sets have been used, where at least six optimisation runs resulted in a common minimum.

The influence of sound radiation due to propeller vibration has been investigated. It has been shown that inclusion of sound radation due to propeller vibration leads to a higher RC virtual damping parameter which reduces axial vibration of the propeller/shafting system, and therefore sound radiation due to propeller vibration. The parameter space has been visualised for cost functions when sound radiation due to propeller vi-

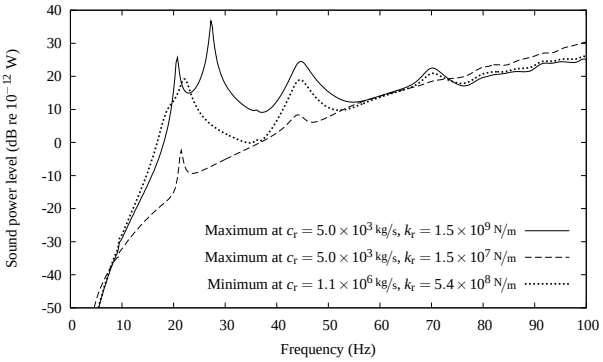

Figure 10: Radiated sound power at the maximum and minimum values of the cost function, when sound radiation due to propeller vibration is considered

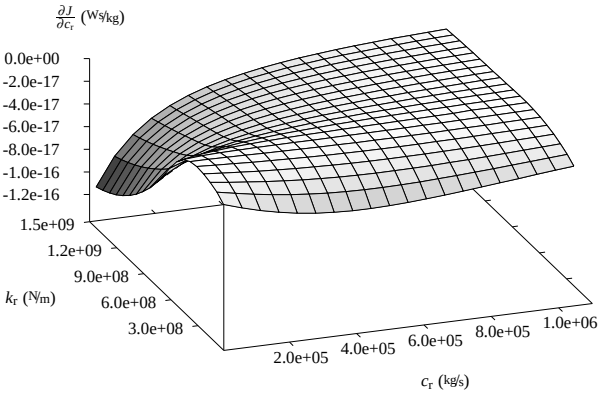

Figure 11: Sensitivity of the cost function when sound radiation due to propeller vibration is considered, with respect to the virtual damping of the RC

bration has been both neglected and included, by keeping one optimum parameter constant.

REFERENCES

S. Amini, P. J. Harris, and D. T. Wilton. *Coupled Boundary and Finite Element Methods for the Solution of the Dynamic Fluid-Structure Interaction Problem*. Springer-Verlag, 1992.

F. B. Belgacem. The mortar finite element method with lagrange multipliers. *Numerische Mathematik*, 84(2):173–197, 1999.

C. A. Brebbia and R. D. Ciskowski. *Boundary Element Methods in Acoustics*. Elsevier Applied Science, New York, 1991.

R. H. Byrd, P. Lu, J. Nocedal, and C. Zhu. A limited memory algorithm for bound constrained optimization. *SIAM Journal on Scientific Computing*, 16(5):1190–1208, 1995.

J. S. Carlton. *Marine Propellers and Propulsion*. Butterworth-Heinemann, Oxford, 1994.

P. G. Dylejko. *Optimum Resonance Changer for Submerged Vessel Signature Reduction*. PhD thesis, School of Mechanical and Manufacturing Engineering, The University of New South Wales, Sydney, Australia, 2008.

P. G. Dylejko, N. J. Kessissoglou, Y. K. Tso, and C. J. Norwood. Optimisation of a resonance changer to minimise the vibration transmission in marine vessels. *Journal of Sound and Vibration*, 300:101–116, 2007.

A. J. H. Goodwin. The design of a resonance changer to overcome excessive axial vibration of propeller shafting. *Institute of Marine Engineers—Transactions*, 72:37–63, 1960.

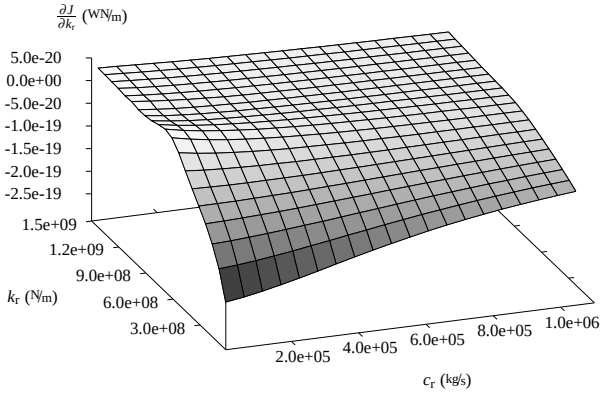

Figure 12: Sensitivity of the cost function when sound radiation due to propeller vibration is considered, with respect to the virtual stiffness of the RC

R. T. Haftka and Z. Gurdal. *Elements of Structural Optimization*. Kluwer Academic Publishers, Boston, 3rd edition, 1992.

S. Marburg. Developments in structural-acoustic optimization for passive noise control. *Archives of Computational Methods in Engineering*, 9(4):291–370, 2002.

T. Mellow and L. Kärkkäinen. On the sound field of an oscillating disk in a finite open and closed circular baffle. *Journal of the Acoustical Society of America*, 118(3):1311–1325, 2005.

S. Merz, R. Kinns, and N. J. Kessissoglou. Structural and acoustic responses of a submarine hull due to propeller forces. *Journal of Sound and Vibration*, 325:266–286, 2009a.

S. Merz, N. J. Kessissoglou, and R. Kinns. Influence of resonance changer parameters on the radiated sound power of a submarine. *Acoustics Australia*, 37:12–17, 2009b.

V. A. Miller and G. J. Davis. Adaptive quadrature on a message-passing multiprocessor. *Journal of Parallel and Distributed Computing*, 14(4):417–425, 1992.

P. M. Morse and K. U. Ingard. *Theoretical Acoustics*. McGraw-Hill, New York, 1968.

C. Norwood. The free vibration behaviour of ring stiffened cylinders. Technical Report 200, DSTO Aeronautical and Maritime Research Laboratory, Melbourne, Australia, 1995.

D. Ross. *Mechanics of Underwater Noise*. Penninsula Publishing, Los Altos, 1987.

K. Svanberg. The method of moving asymptotes – a new method for structural optimization. *International Journal for Numerical Methods in Engineering*, 24(2):359–373, 1987.

K. Svanberg. A class of globally convergent optimization methods based on conservative convex separable approximations. *SIAM Journal on Optimization*, 12(2):555–573, 2002.

Y. K. Tso and C. J. Jenkins. Low frequency hull radiation noise. Technical Report TR05660, Defence Science and Technology Laboratory (Dstl), UK, 2003.

T. W. Wu, editor. *Boundary Element Acoustics*. WIT Press, Southampton, 2000.

O. C. Zienkiewicz and R. L. Taylor. *The Finite Element Method: Solid Mechanics*, volume 2. Elsevier Butterworth-Heinemann, Amsterdam, London, 6th edition, 2005.